LAWRENCE
LIVERMORE
NATIONAL
LABORATORY

LLNL-JRNL-401372

Structure of the Methanol Liquid-Vapor Interface: A Comprehensive Particle-Baesd Simulation Study

I.-F. W. Kuo, C. J. Mundy, M. J. McGrath, J. I. Siepmann

February 14, 2008

Journal of Physical Chemistry C

Disclaimer

This document was prepared as an account of work sponsored by an agency of the United States government. Neither the United States government nor Lawrence Livermore National Security, LLC, nor any of their employees makes any warranty, expressed or implied, or assumes any legal liability or responsibility for the accuracy, completeness, or usefulness of any information, apparatus, product, or process disclosed, or represents that its use would not infringe privately owned rights. Reference herein to any specific commercial product, process, or service by trade name, trademark, manufacturer, or otherwise does not necessarily constitute or imply its endorsement, recommendation, or favoring by the United States government or Lawrence Livermore National Security, LLC. The views and opinions of authors expressed herein do not necessarily state or reflect those of the United States government or Lawrence Livermore National Security, LLC, and shall not be used for advertising or product endorsement purposes.

Structure of the Methanol Liquid-Vapor Interface: A Comprehensive Particle-Based Simulation Study

I-F. William Kuo,[1] Christopher J. Mundy,[2] Matthew J. McGrath,[3] J. Ilja Siepmann[4]*

[1]Computational Chemical Biology, Lawrence Livermore National Laboratory

P.O. Box 808, Livermore, CA 94551

[2]Fundamental and Computational Sciences Directorate, Pacific Northwest National Laboratory

P.O. Box 999, Richland, WA 99352

[3]Universite de Dschang, Cameroon

B.P. 217, Dschang, Cameroon, West Africa

[4]Departments of Chemistry and of Chemical Engineering and Materials Science, University of Minnesota

207 Pleasant Street SE, Minneapolis, MN 55455-0431

RECEIVED DATE: February 12, 2008

* E-mail: kuo2@llnl.gov

ABSTRACT

This research addresses a comprehensive particle-based simulation study of the structural, dynamic, and electronic properties of the liquid-vapor interface of methanol utilizing both *ab initio* (based on density functional theory) and empirical (fixed charge) models. Numerous properties such as interfacial width, hydrogen bond populations, dipole moments, and correlation times will be characterized with identical schemes to draw useful conclusions on the strengths and weakness of the proposed models for the interface of neat methanol. Our findings indicate that all models considered in this study yield similar results for the radial distribution functions, hydrogen bond populations, and orientational relaxation times. Significant differences in the models appear when examining both the dipole moments and surface relaxation near the aqueous liquid-vapor interface. Here, the density functional theory interaction potential predicts a significant decrease in the molecular dipole moment and slight expansion in the oxygen-oxygen distance as one approaches the interface.

KEYWORDS: air-methanol interface, liquid-vapor interface, hydrogen bond, surface relaxation, methanol

I. Introduction:

Hydrogen bonding fluids have been the focus of intense study utilizing molecular simulations. Besides the clear connection of hydrogen bonding fluids to important processes in biology, the nature of hydrogen bonding fluids remains an active area of fundamental research. Moreover with the recent advances in fast electronic structure algorithms in conjunction with high-performance computing, it is not uncommon to perform 10-20 picosecond trajectories using density functional theory (DFT) based interaction potentials. Moreover, it has been shown that we can go beyond homogeneous systems and study the heterogeneous liquid-vapor interfaces in aqueous systems. Thus, in the past few years, there has been a re-examination of simulation protocol and the sensitivity of this protocol on the underlying structure and dynamics of aqueous systems. To this end, there have been numerous studies on the effects of basis set, functional, and sampling methods to probe the sensitivity and reproducibility of structural and dynamical quantities in aqueous systems. More recently there has been a strong effort to include the effects of London dispersion into DFT interaction potentials. Until recently, there was no conclusive study that DFT interaction potentials could produce a stable liquid phase. The conventional wisdom that is now emerging is that for aqueous systems, the liquid density is terribly underestimated (roughly 20%) using DFT in conjunction with standard gradient corrected exchange and correlation functionals. Unfortunately, the understanding of the sensitivity of the liquid density to hybrid exchange correlation functionals is still computationally prohibitive. Probing the sensitivity of liquid density to the effects of London dispersion is still an active area of research. However, we can indirectly probe the consequence of lack of London dispersion by performing simulations of liquid methanol. Methanol is the simplest of alcohols, and the most similar alcohol to water with a single hydrogen being replaced by a methyl group. It is also well known that methyl-methyl interactions need a strong component of dispersion in order to be modeled correctly. Moreover, the interaction potential of a variety of alcohols is known to reproduce the experimental liquid-vapor coexistence curve, and heats of vaporization to within 2%, a benchmark that no empirical model for water has yet achieved. In this study we utilize the so-called united atom transferable interaction potentials for phase equilibria (TraPPE-UA) to benchmark methanol simulations (both bulk and the liquid-vapor interface) against DFT interaction potentials utilizing both Perdew Burke Ernzerhof (PBE) and Becke-Lee-Yang-Parr (BLYP) exchange and correlation functionals. Direct comparisons of structure, liquid densities, and hydrogen bonding populations will be made to experiment (when available) and fixed charge TraPPE-UA on equal footing in order to understand the performance of DFT interaction potentials to systems where both hydrogen bonging and dispersion are known to be important.

II. Simulation Details:

Molecular Dynamics Simulations

First principles molecular dynamics simulations were performed using the software suite CP2K[1] where the energy and force was obtained from the QuickStep module.[2] The QuickStep module contains a fast electronic structure code based on the Kohn-Sham (KS) formulation of DFT.[3] For these calculations, a dual basis set of Gaussian Type Orbitals (TZV2P) with auxiliary plane waves expanded up to 280 Ry was used to describe the valence states. The core states are described through the GTH pseudopotential.[4] The calculations were performed using both the BLYP[5,6] and PBE[7] exchange and correlation functionals due to their ubiquitous use in studying hydrogen bonded fluids. The amount of vacuum (36 Å) was chosen such that this simulation was converged with respect to this parameter.[8] Nosé-Hoover thermostats[9,10] were attached to every degree of freedom, with a thermostatting frequency of 2000 cm^{-1} to ensure thermal equilibrium over the entire MD trajectory.

Our DFT simulation of the methanol liquid-vapor interface was performed on 120 methanol molecules in a simulation cell of dimension 15 Å x 15 Å x 73 Å. The distance between the two free interfaces in the z direction was approximately 36 Å. A total of 15ps (5ps of equilibration + 10ps of production) of molecular dynamics simulation was performed using the two different functionals with the same initial starting configuration obtained from a equilibrated classical Monte Carlo simulations based on the TraPPE-UA force field.[11] In addition, two bulk methanol simulations were performed at ambient condition for 30ps total (5ps of equilibration + 25ps of production). Due to potential finite size effects, for the bulk methanol simulation, the simulation cell dimension is (16.3439 Å) containing 64 methanol molecules.

Monte Carlo Simulations

Interfacial structural properties for TraPPE-UA methanol were calculated using Monte Carlo simulations combining the Gibbs ensemble (GEMC) and coupled-decoupled configurational-bias (CBMC) techniques.[12,13] The simulation setup for the interfacial calculations is similar to that used previously by some of the authors for studying the vapor-liquid interface of pure water and water/1-butanol mixtures.[14,15] Here we utilized an elongated liquid box containing initially 800 methanol molecules with dimensions 30 Å x 30 Å x 120 Å, and a vapor box with initially 100 helium atoms to ensure a constant pressure. In addition to the external pressure and temperature, the MC simulations maintain as constants the overall numbers of methanol and helium molecules and the interfacial area of the liquid box. The initial configuration of the liquid slab was taken from an independent NVT

simulation of a bulk liquid at 300 K with box dimensions 30 Å x 30 Å x 30 Å, which yields a liquid density of 0.79 g/cm^3. The final configuration of this system was replicated in the z-direction to generate a liquid slab with dimensions 30 Å x 30 Å x 60 Å. This slab was placed in the center of the liquid box for the GEMC simulations allowing for approximately 60 Å of vacuum between the two vapor-liquid interfaces after periodic boundaries were implemented. Equilibration of the slab system at 300 K and 1 atm took place through box volume changes (the volume of the vapor box was allowed to change while keeping all cell lengths equal, but only the z-dimension of the liquid slab box was allowed to fluctuate), CBMC swap moves of helium and water molecules between the two boxes, rotation and translation of water molecules, and translation of helium atoms. A total of 4 independent simulations were run, each consisting of more than 5 x 10^4 MC cycles for equilibration (where one MC cycle consists of 900 randomly selected MC moves), and using 10^5 MC cycles for production. Properties were calculated by averaging over all 4 independent simulations. The bulk properties without an interface were computed by using 800 TraPPE-UA methanol molecules in the isobaric-isothermal ensemble.[16,17] A production period of 10^5 Monte Carlo cycles followed 5 x 10^4 equilibration cycles.

III. Results and Discussion:

Radial distribution functions

The radial distribution functions (RDF) for oxygen-oxygen, oxygen-hydrogen, carbon-oxygen, and carbon-carbon pairs (i.e. $g_{OO}(r)$, $g_{OH}(r)$, $g_{CO}(r)$, and $g_{CC}(r)$ respectively) were calculated for the TraPPE-UA, BLYP, and PBE interaction potential for bulk methanol are shown in **Figure 1**. From **Figure 1**, it can be seen that there is good agreement overall between all the interaction potential employed in this study though slight differences can be gleamed. First, for the oxygen-oxygen pair distribution function ($g_{OO}(r)$), the two DFT potentials predicts a well defined first solvation shell when compared to TraPPE-UA due to the lower value at the minimum of the first solvation shell. Similarly, if we look at the oxygen-hydrogen pair distribution function ($g_{OH}(r)$) and observed the first peak and minimum due to intermolecular interaction, we again noticed that the BLYP and PBE gives a slightly more structure solvation shell as judged by its peak height and minimum. The overstructuring of the RDF for both exchange and correlation functionals compared to TraPPE-UA is analogous to the overstructuring found in liquid water.[18] In contrast, carbon-oxygen and carbon-carbon pair distribution functions ($g_{CO}(r)$ and $g_{CC}(r)$) does not show overstructuring for either DFT based potential when compared to that of TraPPE-UA. Though the RDF for BLYP and PBE are similar, it can be seen in **Figure 1**, that PBE produces a slightly more structured $g_{OO}(r)$ when compared to BLYP. When compared to pulsed neutron diffraction

data from Soper et. al.,[19,20] both the RDFs for BLYP and PBE produce an over structured first solvation shell. Specifically, the computed RDF for the peak of the first solvation shell for BLYP and PBE is roughly 4, whereas experiments suggest it should be around 3. Similar overstructuring is also observed in a study using classical many-body interaction potential with out-of-plane isotropic polarizability.[21] Likewise, the first minimum is more pronounce in our BLYP and PBE simulation when compared to experimental results. Though the methanol was simulated at 300K here, it is apparent that the RDF obtained here is more structured then previous DFT studies using plane-wave basis and BLYP exchange-correlation functional for 32 and 64 methanol molecules at 293 K.[22,23] This discrepancy is likely due to the different simulation protocol utilizing, namely Car-Parrinello (CP) versus Born-Oppenheimer (BO) dynamics. It has been shown that one can obtain agreement between the two methods for liquid water, but the details are sensitive to length of simulation, value of fictitious mass, density cut-off, and temperature control.[18]

Interfacial width

A converged density profile is usually a sign of a stable interfacial system. In order to compare interfacial profiles amongst the different models and sampling protocols used in this study, we compute the interfacial width from a standard fit of the density profile in the z dimension, $\rho(z)$, to a hyperbolic tangent function of the form:

$$\rho(z) = \frac{1}{2}(\rho_l + \rho_v) - \frac{1}{2}(\rho_l - \rho_v)\tanh\left(\frac{z - z_{GDS}}{\delta}\right).$$

Here ρ_l and ρ_v correspond to the density of liquid water and water vapor, respectively, z_{GDS} is the Gibbs dividing surface (i.e. the z value at $0.5\rho_l$ if ρ_v is negligible), and δ is an interface thickness parameter. The parameters that yielded the best fit to the simulated density profiles are shown in **Table 1**, and ρ_v was taken to be zero (*e.g.* less than 10^{-7}g/cm^3). Plots of the raw data and fits to the density profiles are shown in **Figure 2**. From **Table 1**, the TraPPE-UA potential gives a bulk density of 0.774 g/cm^3 that is in extremely good agreement to the experimental density of 0.780 g/cm^3. For the BLYP and PBE interface, we found that the fitted bulk density to be 0.670 g/cm^3 and 0.689 g/cm^3 respectively, which underestimates experimental value by around 10% to 15%. Comparison between BLYP and PBE reveals that PBE yields a higher bulk density when compared to BLYP which can be seen in the fitted value for ρ_l in **Table 1**. The higher density of PBE is also found in our recent studies of water, and we conjecture that PBE may yield densities that are higher than BLYP for all hydrogen bonded liquids.[24] Though the interfacial thickness parameter (δ) was computed for all three interfaces, the value obtained for BLYP and PBE are plagued with a large error due to a lack of spatial sampling resulting from the

relatively short simulation time. This is evident in the raw density profile in **Figure 2** for BLYP and PBE that is dominated by noise due to a lack of spatial sampling during the final 10 ps over which the analysis was performed. Thus, any fitting procedure would have to be based on a weighted fit that underscores the uncertainty in the spatial sampling. However, one salient feature unambiguously clear from **Figure 2**, is that BLYP and PBE does not reproduce the bulk density of liquid methanol.

Dipole moments and Molecular States

Molecular dipole moments computed for the BLYP and PBE interactions are plotted in **Figure 3**. The individual dipole moments for the BLYP and PBE interaction potential were computed via the Wannier centroid analysis where the seven centers of electron charge (five bonding and two nonbonding-pairs) are given a value of $-2e$, reflecting the nature of the spin restricted calculation.[25,26] For the bulk, the distribution of molecular dipole (inset of **Figure 3**) is in good agreement with previous liquid methanol simulations using BLYP functional and plane-wave basis[22,23] and a classical empirical interaction potential with out-of-plane isotropic polarizability.[21] In addition, we have computed the molecular dipole moment for the methanol interface and plotted the average dipole moment as a function of interfacial coordinate in **Figure 3**. For the methanol slab both BLYP and PBE yield an average dipole moment at the interior of the interface that fluctuates between 2.6 D and 2.9 D. Overall, the average dipole for PBE is slightly higher then those found for BLYP which is in accordance with a more structured RDF that was discussed previously. As the air-methanol interface is approached, the dipole moment exhibits similar behavior to studies of the air-water[14,27,28] –methanaol[21] interface where we see a clear drop of the molecular dipole moment approaching that of its computed monomeric value of 1.73 D.[22]

In addition, we utilize the method developed by Vuilleumier and Sprik[29] to compute the effective molecular orbitals and energies for each methanol molecule in our BLYP and PBE interface. **Figure 4** shows the average molecular eigenvalue for the highest occupied molecular orbital (HOMO) as a function of the interfacial coordinate. Similar to results obtained for the aqueous liquid-vapor interface, we see an increase in the HOMO for methanol in the vicinity of interfacial region relative to the bulk. This points to the potential of interface, on average, to be more chemically reactive and implication towards heterogeneous chemistry.

Hydrogen bond populations

Recent experiments vibrational and X-ray absorption spectroscopy suggests that the surface of methanol should have different hydrogen bonding topology or strength relative to the bulk.[30-32] Using atomistic methods as employed here, it is possible for us to compare the different hydrogen bonding

populations present at the interior and surface of the interfacial system. A previous detailed study of the hydrogen bond topology of aqueous systems using a variety of hydrogen bonding criteria have shown that resulting populations although being quantitatively different show the same qualitative trend when one compares the bulk to the interface.[14] With this in mind, we will employ two simple hydrogen bond definitions to analyze the results of the simulations presented here, namely the commonly used hydrogen bond criteria of standard distance ($\mathbf{r}$(OH) = 2.27Å) and angle ($\angle$(OHO) = 140°) and that proposed by Wernet et al.[33] The hydrogen bond populations computed for methanol in the vicinity of the interface ("surface") and bulk region ("interior") of the slab are presented in **Table 2** and **Table 3**. The division between interior and surface regions is indeed arbitrary. We choose a dividing plane in the *xy* dimension where a *z* value of 2δ below the Gibbs dividing surface is considered the interior. This choice is conservative ensuring that the interior region of our water slab is not influenced by the presence of the interface. Moreover, this choice will allow for direct comparison to condensed phased calculations. By selecting a hydrogen bonding criteria, we were able to partition each methanol molecule for a particular region into different species as characterized by its number of "donor" and "acceptor" hydrogen bonds. A fully hydrogen bonded methanol molecule will have 1 "donor" and 2 "acceptor" hydrogen bonds and designated as (1A,2D).

In **Table 2** and **Table 3**, the hydrogen bond populations are tabulated for BLYP, PBE, and TraPPE-UA interaction potential. Though the different hydrogen bonding criteria and different interaction potential give slightly different populations, it can be seen that the predominant population for both the interior and surface region is the (1A,1D) as would be expected. This is in contrast to the hydrogen bond population for surface water which have distinct hydrogen bonding populations relative to the interior.[14,28] Interestingly, for methanol we observe no statistical difference between hydrogen bond populations at the surface and interior molecules regardless of the interaction potential that is used.

Surface Relaxation

A very interesting phenomena measured by the EXAFS experiment is the surface relaxation in the vicinity of the interface that is manifested as a 4.6% contraction in the oxygen-oxygen distance in the surface region of the interfacial system.[31] Surface relaxation is a well known phenomena in solids where the large surface energy due to unsatisfied bonds is compensated for by a reduction in interlayer spacing as one approaches the solid-vacuum interface. However, quantifying surface relaxation in the case of a liquid is not as straight forward as in a solid, and thus one must rely on multiple analyses. In order to quantify the nature of the surface relaxation for the methanol liquid-vapor interface, we have computed the average oxygen-oxygen distance for all simulations performed in this study. The average oxygen-

oxygen distance is shown in **Figure 5** and was computed for first solvation pair as defined by the first minimum of the radial distribution function $g_{OO}(r)$, namely 3.5 Å. For comparison, it was determined that the average oxygen-oxygen distance for bulk methanol at 300 K was 2.8246 Å, 2.765 Å, and 2.8135 Å for BLYP, PBE, and TraPPE-UA interaction potential respectively. For analysis purposes, the trajectories were subdivided into multiple blocks to aid in determining the level of uncertainty.

In previous study of aqueous liquid-vapor interface, different empirical force fields were tested and the average oxygen-oxygen distance was computed in order to quantify surface relaxation.[14,34] It was found that when using interaction potentials with no polarization or only containing in-plane polarization, a surface contraction in the vicinity of the interface is found.[34] This finding is contrary to both experiment[31] and simulations using DFT or empirical interaction potentials containing out-of-plane isotropic polarizability.[21] In **Figure 5**, we can see that TraPPE-UA potential does not produce any observed surface expansion or contraction in line with what is expected with an empirical fixed charge interaction potential. One should note that the average oxygen-oxygen distance as a function of the interfacial coordinate for both BLYP and PBE exchange and correlation functionals fluctuates in the interior of the slab greater then any observed shift for the oxygen-oxygen distance in the vicinity of the interface. Thus, we do not observe a surface contraction the methanol liquid-vapor interface contrary to EXAFS experiments by computing the average oxygen-oxygen distance.

Surface Orientation

The invariance of the oxygen-oxygen distance as a function of interfacial depth is surprising because methanol tends to orient itself in a very systematic way in the vicinity of interface. As can be seen in **Figure 6**, using the carbon-oxygen bond as a molecular vector, we have computed the angular distribution of methanol relative to the surface normal as a function of interfacial depth for TraPPE-UA, BLYP, and PBE interaction potential. Although the distribution for BLYP and PBE is not as smooth as those obtained using TraPPE-UA, all three interaction potential points to a highly structured interfacial region where methanol molecules at the interface are highly correlated. From **Figure 6**, it can be seen that methanol at the interface tends to have its polar hydroxyl groups orient inward towards the bulk region while the methyl group are oriented to point toward the vacuum. This orientation leads to a highly structured and packed interfacial region that should decrease the average oxygen-oxygen distance in accordance with experiment.[31]

Using the same carbon-oxygen bond as a molecular vector and surface normal, molecular reorientation was probed using time correlation function based on second rank Legendre poloynomial analogous to the method applied to studies of aqueous interfaces.[14] The slab was partition into interior

and surface region as mentioned in previous sections but care was taken to account for molecular diffusivity across the imaginary plane that separate interior/surface region. The correlation function $C_2(t)$ was only computed if the methanol molecule does not diffuse across the imaginary plane that separates the interior/surface region of the slab. The correlation functions for surface reorientation are shown in Figure 7. Like previous studies of aqueous interfaces, rotational dynamics at the methanol interface appears to be faster than the corresponding interior region of the slab. This is conjunction with Figure 6 shows that the topmost layer of methanol behaves like a spinning top with the hydrogen bonds acting as an anchor and the methyl group freely to move about.

IV. Conclusions:

We have presented a particle-based simulation study of the methanol liquid-vapor interface. In particular, we have provided a comparison between classical empirical potentials (TraPPE-UA) with DFT based interaction potential (BLYP and PBE) and compared our results to experiment when available for this important system. Our findings indicate that all structural and electronic properties are in close agreement between the different interaction potentials. This is encouraging given the dramatic differences in the details of the interaction potential. In particular, the agreement of the surface populations of hydrogen bonded species seems to be independent of the precise nature of the interaction potential. Of notable exception are extrapolated bulk densities where BLYP and PBE significantly underestimate the bulk density. We saw a pronounced decrease in molecular dipole moment for BLYP and PBE near the surface, suggesting a dramatic loss of interaction energy due to charge reorganization occurred in the BLYP and PBE model. In conjunction, we have shown that the surface is highly structured with at least one highly oriented layer of methanol. It is this highly structured surface where methanol molecules are aligned to expose the hydrophobic methyl group to the vacuum that could account for the measured decrease in the oxygen-oxygen distance from EXAFS experiments.

ACKNOWLEDGMENT Part of this work was performed under the auspices of the U.S. Department of Energy by Lawrence Livermore National Laboratory under Contract DE-AC52-07NA27344 and financial support from the National Science Foundation (CTS-0138393, CHE-0431312, and CHE-0209719), EMSI (ITR-0428774), and DOE Computational Science Graduate and 3M Foundation Fellowships (M.J.M.) is gratefully acknowledged. We would like to thank R. Saykally, Jared Smith, and Chris Cappa for stimulating discussions, and the LLNL Computing staff for their help. Computer

resources were provided by Livermore Computing and Minnesota Supercomputing Institute.

Table 1. Fitted density profile parameters for methanol liquid-vapor interface.

	BLYP	PBE	TraPPE-UA
ρ_l (g/cm^3)	0.670	0.689	0.774
δ (Å)	4.16	2.918	2.61
z_{GDS} (Å)	20.89	20.24	29.16

The density profile was fitted to $\rho(z) = \frac{1}{2}(\rho_l + \rho_v) - \frac{1}{2}(\rho_l - \rho_v)\tanh\left(\frac{z - z_{GDS}}{\delta}\right)$ with the center of mass shifted to $z = 0$ for the fitting.

Table 2. Hydrogen bond populations (D=donor: A=acceptor) for the interior region of the slab.

BLYP PBE TraPPE-UA	0D		1D	
0A	1.467 0.720 1.965	1.432 0.677 1.700	8.356 7.325 12.391	8.187 7.133 11.724
1A	3.926 2.328 7.091	3.702 2.113 6.227	80.748 83.008 73.222	81.173 83.429 74.761
2A	0.049 0.015 0.270	0.066 0.002 0.217	5.454 6.604 5.055	5.441 6.647 5.364

The boundary between "interior" and "surface" is defined by an arbitrary plane in the *xy* dimension at $z = 2\delta$ below the Gibbs dividing surface. For the comparison of hydrogen bond populations, a δ value of 2.61Å was use for all three interaction potential. This conservative choice will ensure that computed hydrogen bond population at the interior of the methanol slab will have no residual effects caused by the presence of the interface which allows for direct comparison to condensed phase simulation. For each hydrogen bonding species (i.e. [0D,0A], [0D,1A], etc…), the first columns represents hydrogen bond population using standard distance ($\mathbf{r}$(OH) = 2.27Å) and angle ($\angle$(OHO) = 140°) cutoff criteria while the second column represents hydrogen bond populations using the Wernet[33] criteria.

Table 3. Hydrogen bond populations for the surface region of the slab.

BLYP PBE TraPPE-UA	0D		1D	
0A	3.866 2.975 2.613	3.852 2.956 2.321	9.128 9.241 13.200	9.009 9.062 12.493
1A	3.889 1.606 7.275	3.907 1.381 6.357	80.813 82.686 72.473	80.961 83.040 74.160
2A	0.057 0.038 0.224	0.041 0.034 0.182	2.246 3.453 4.211	2.229 3.526 4.483

The criteria for “interior” versus “surface” water is defined in Table 2.

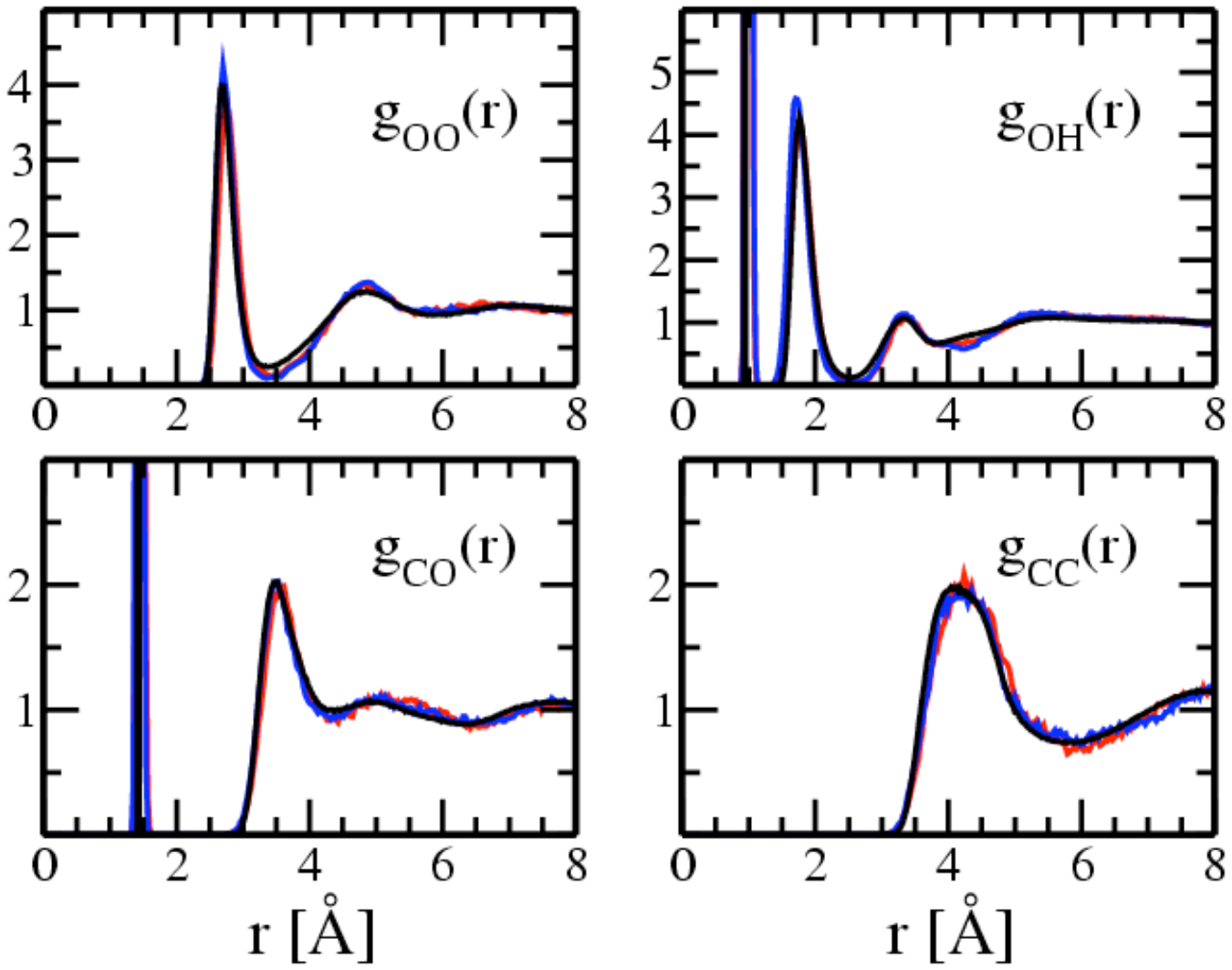

Figure 1. The radial distribution functions (RDF) for liquid methanol at 300K. A bin width of 0.02 Å was used. TraPPE-UA, BLYP, and PBE results are shown *black*, *red*, and *blue* respectively.

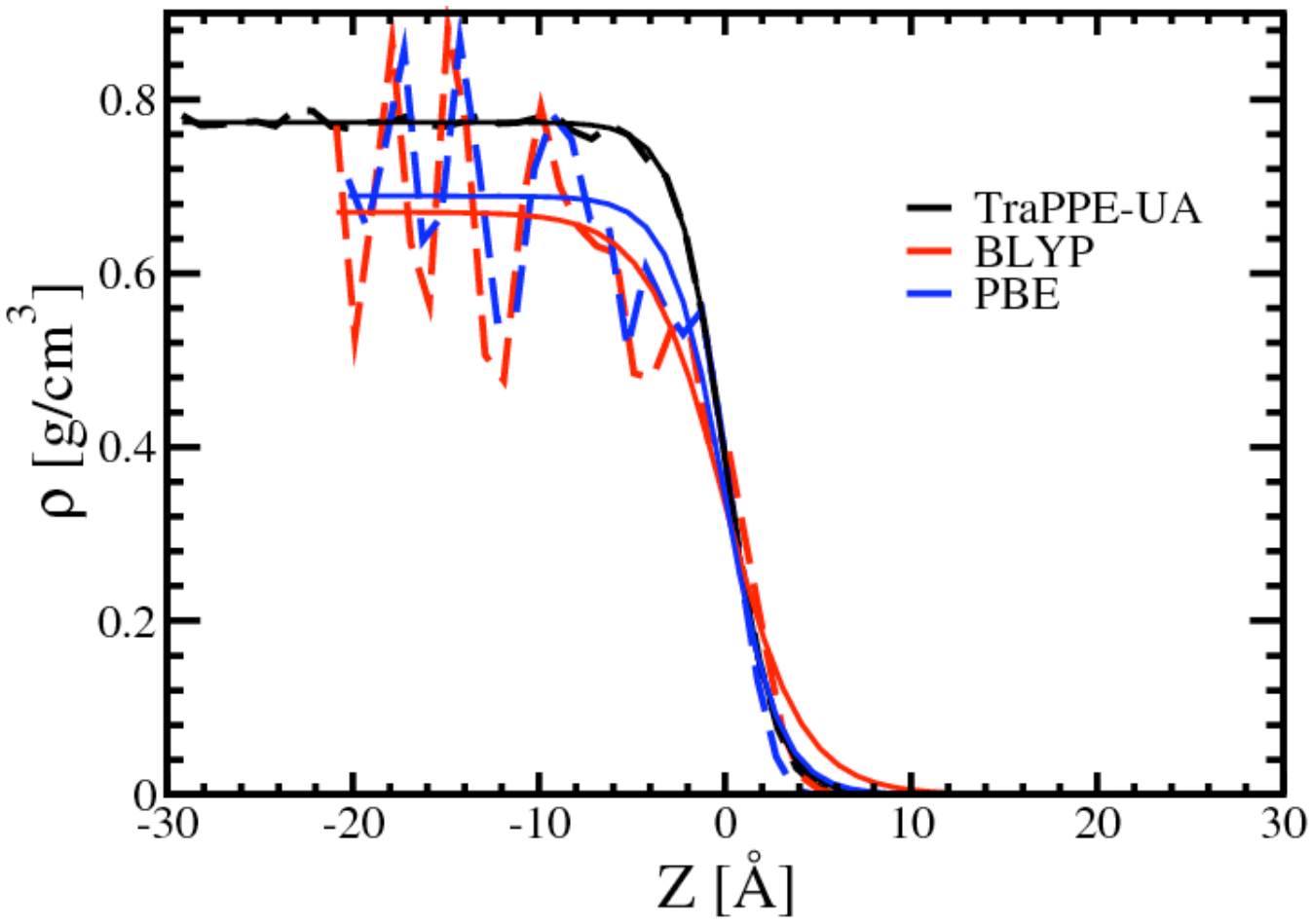

Figure 2. Density profile for liquid-vapor of methanol using different interaction potentials. All interfaces are shifted so that the GDS is located at 0.0Å. The dashed and solid lines show the raw data and their tanh fit respectively.

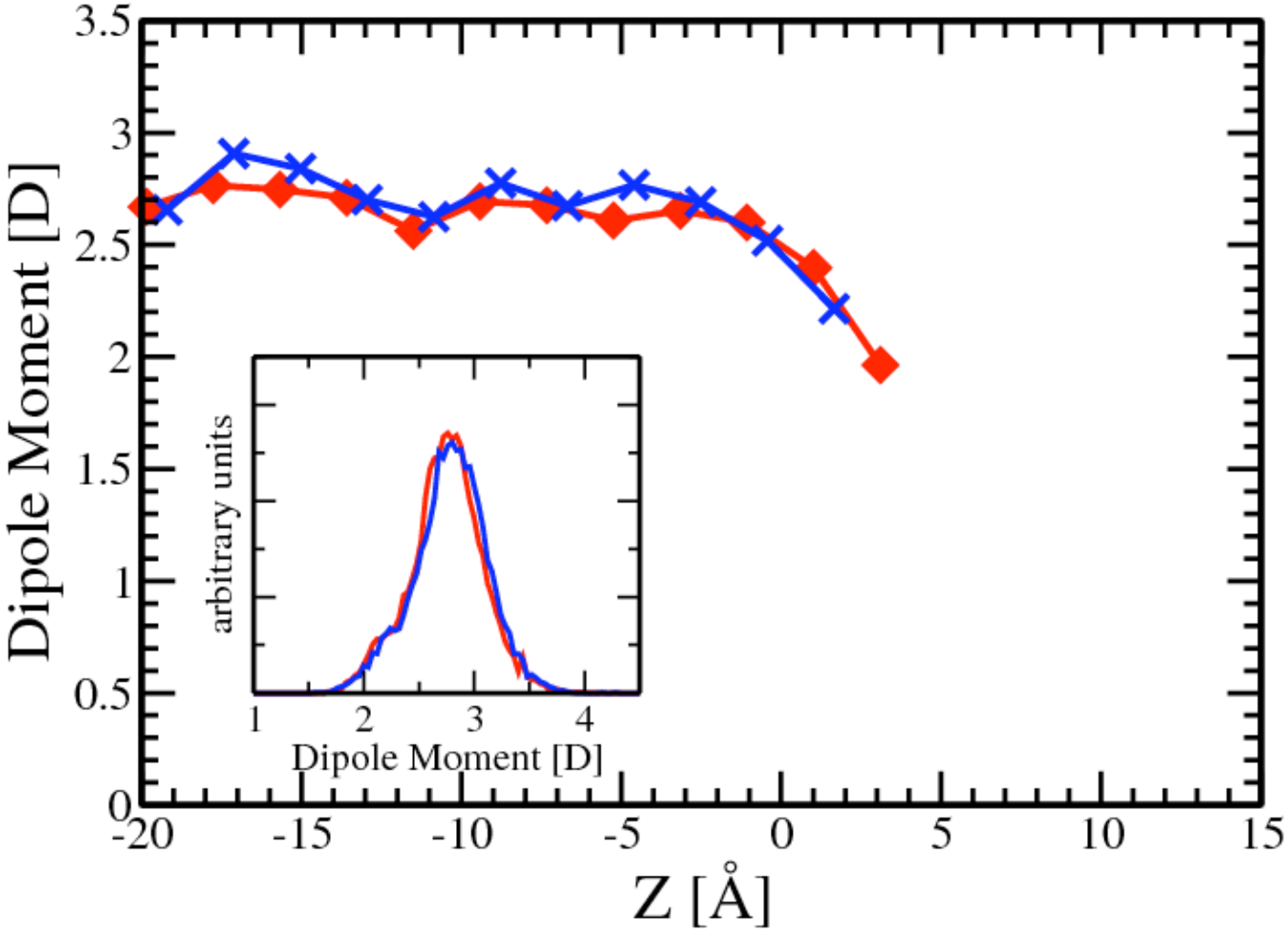

Figure 3. Molecular dipole moment as a function of slab depth and in the inset, the dipole moment distribution for bulk methanol. All interfaces are shifted so that the GDS is located at 0.0Å. Results for BLYP are shown in *red* and PBE results are shown in *blue*.

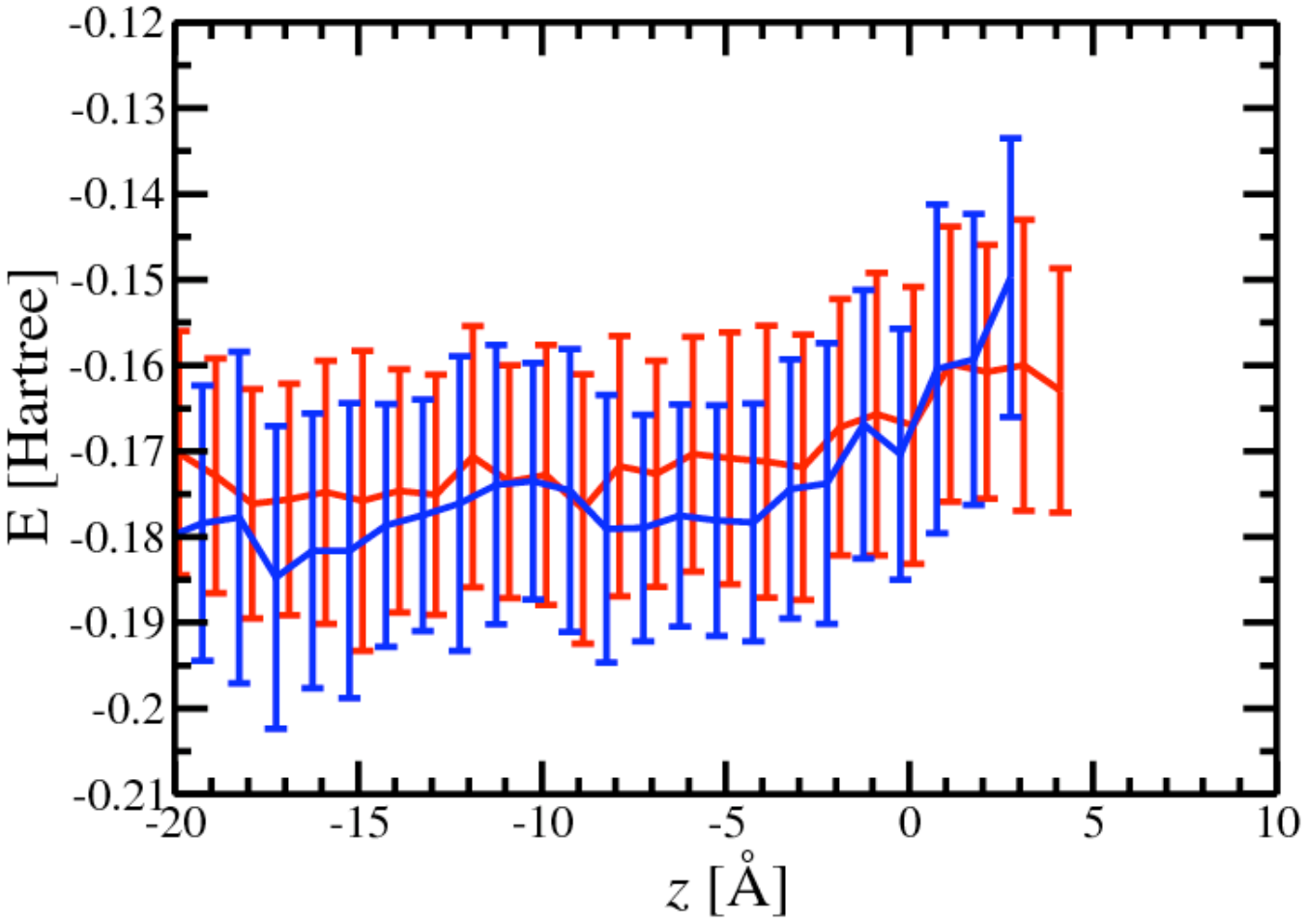

Figure 4. Effective molecular energies for each methanol molecule as a function of interfacial depth. All interfaces are shifted so that the GDS is located at 0.0Å. Results for BLYP are shown in *red* and PBE results are shown in *blue*.

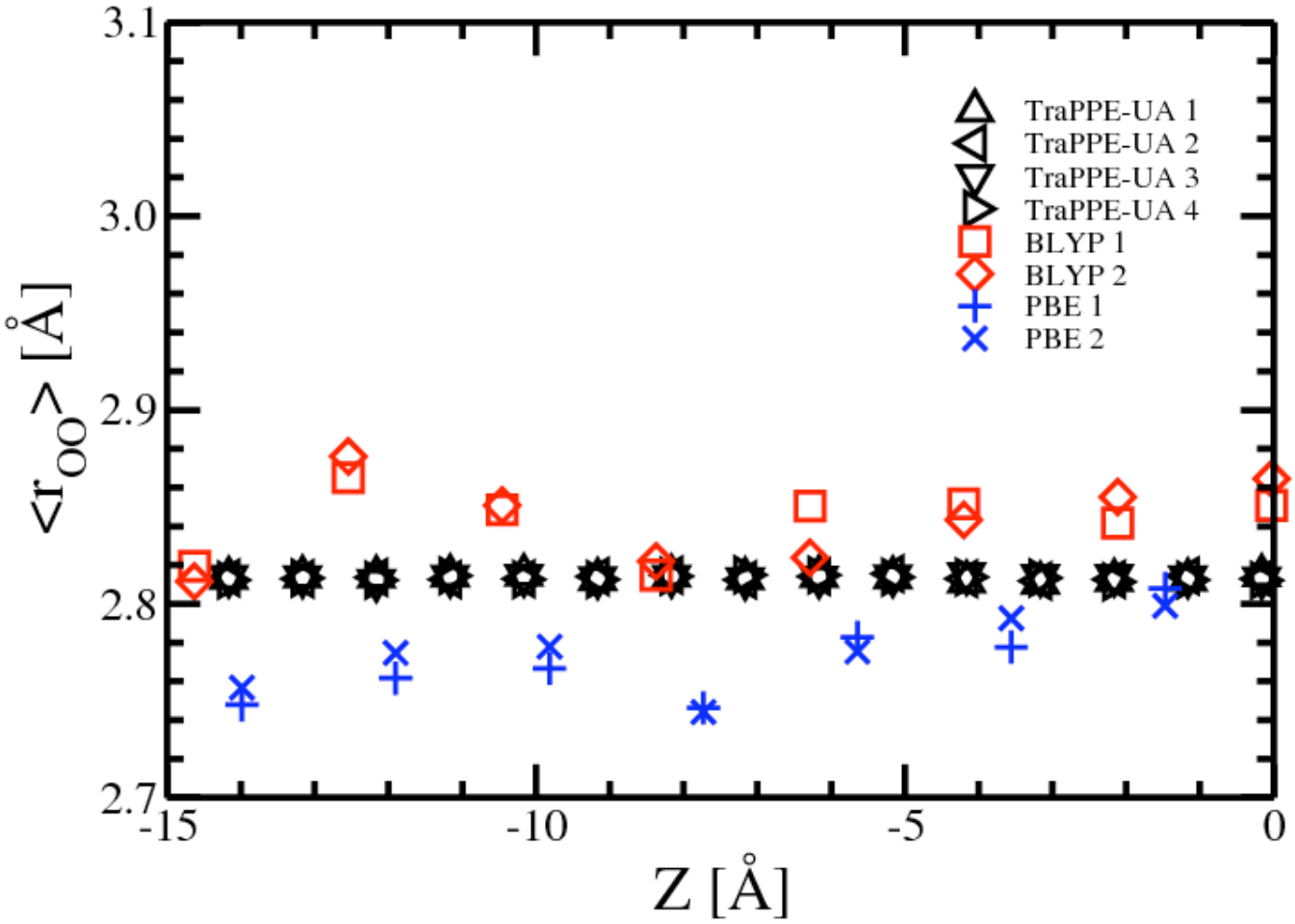

Figure 5. Average oxygen-oxygen distance as a function of depth. All interfaces are shifted so that the GDS is located at 0.0Å. For analysis purposes, the trajectories were subdivided into multiple blocks to aid in determining the level of uncertainty.

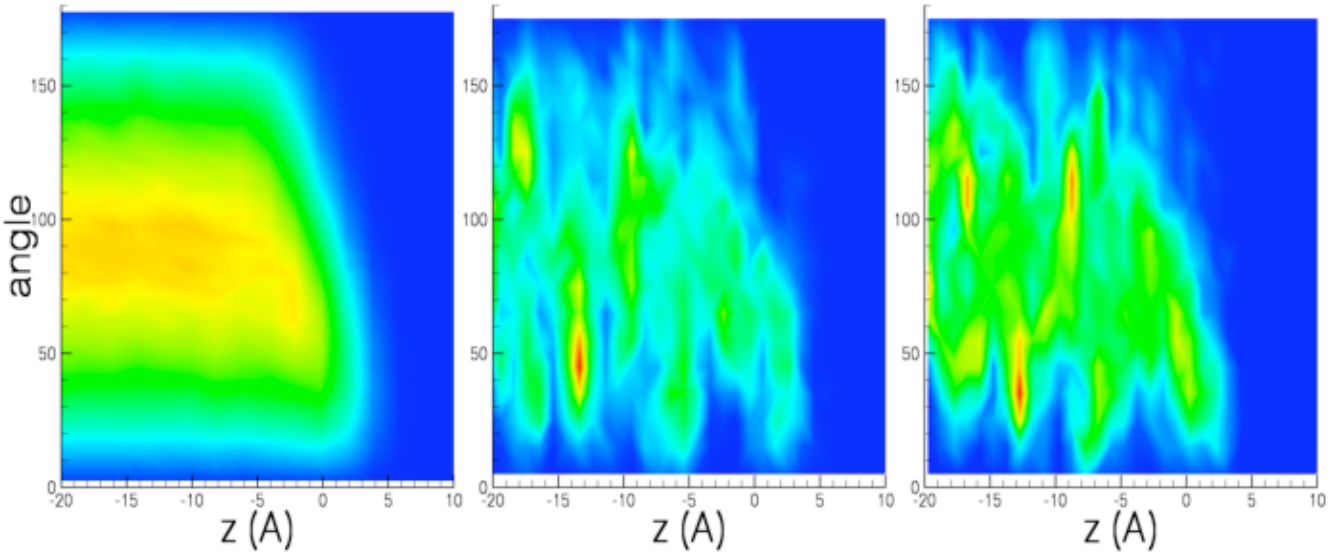

Figure 6. Orientational order of methanol near the interface for TraPPE-UA (left), BLYP (middle), and PBE (right). The angle θ is defined as the angle between the O-C vector and the surface normal *z*. All the interface are shifted so that the GDS is at 0 on the z-axis.

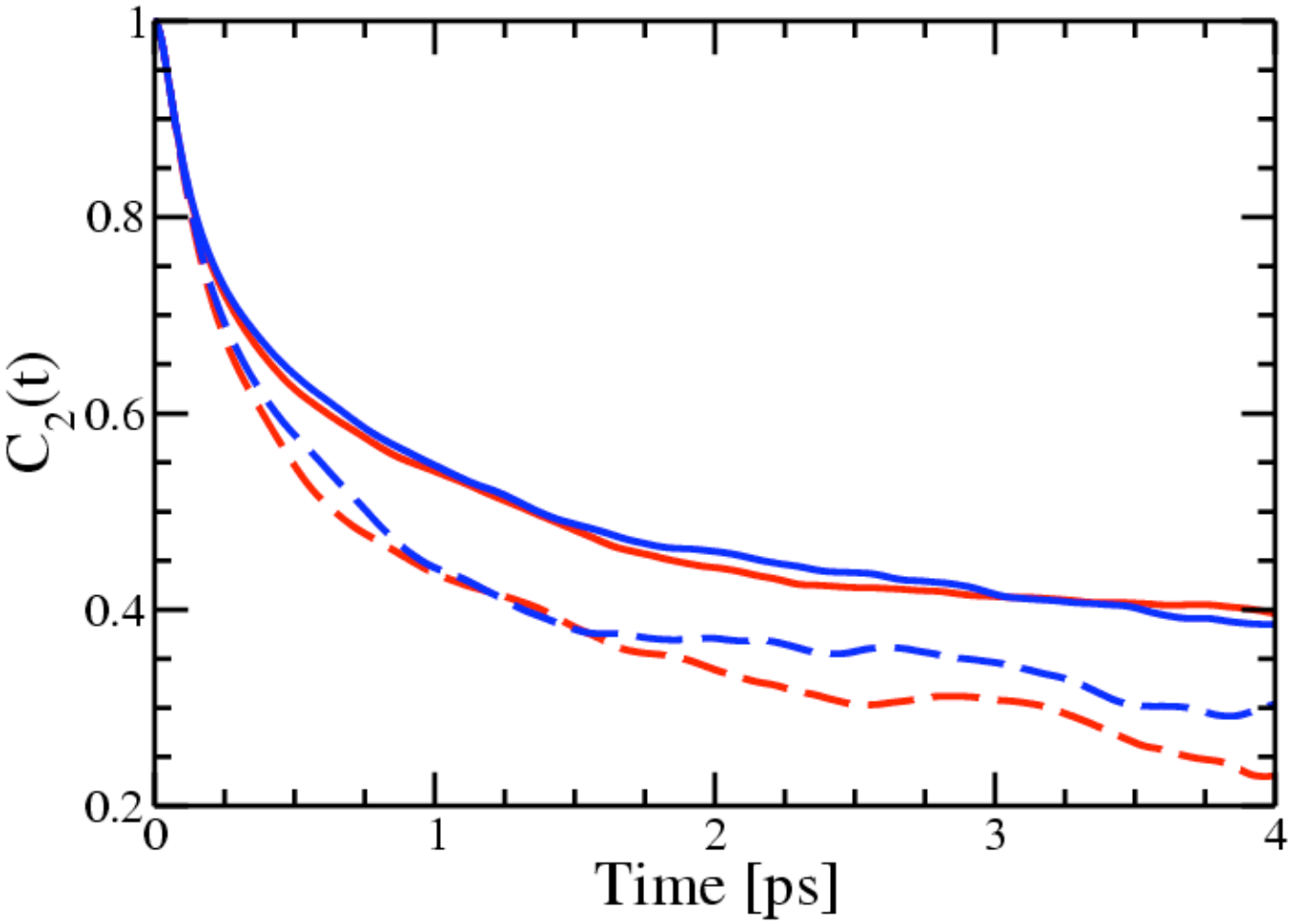

Figure 7. Second rank rotational correlation time for methanol at the surface (*dashed lines*) and interior (*solid lines*) of the slab. Results for BLYP are shown in *red* and PBE results are shown in *blue*.

REFERENCES

(1) CP2K. http://cp2k.berlios.de.

(2) VandeVondele, J.; Krack, M.; Mohamed, F.; Parrinello, M.; Chassaing, T.; Hutter, R. *Comput. Phys. Commun.* **2005**, *167*, 103.

(3) Lippert, G.; Hutter, J.; Parrinello, M. *Mol. Phys.* **1997**, *92*, 477.

(4) Goedecker, S.; Teter, M.; Hutter, J. *Phys. Rev. B* **1996**, *54*, 1703.

(5) Becke, A. D. *Phys. Rev. A* **1988**, *38*, 3098.

(6) Lee, C.; Yang, W.; Parr, R. G. *Phys. Rev. B* **1988**, *37*, 785.

(7) Perdew, J. P.; Burke, K.; Ernzerhof, M. *Phys. Rev. Lett.* **1996**, *77*, 3865.

(8) Mundy, C. J.; Kuo, I. F. W. *Chem. Rev.* **2006**, *106*, 1282.

(9) Hoover, W. G. *Phys. Rev. A* **1985**, *31*, 1695.

(10) Nose, S. *J. Chem. Phys.* **1984**, *81*, 511.

(11) Chen, B.; Potoff, J. J.; Siepmann, J. I. *J. Phys. Chem. B* **2001**, *105*, 3093.

(12) Panagiotopoulos, A. Z. *Mol. Phys.* **1987**, *61*, 813.

(13) Panagiotopoulos, A. Z.; Quirke, N.; Stapleton, M.; Tildesley, D. J. *Mol. Phys.* **1988**, *63*, 527.

(14) Kuo, I. F. W.; Mundy, C. J.; Eggimann, B. L.; McGrath, M. J.; Siepmann, J. I.; Chen, B.; Vieceli, J.; Tobias, D. J. *J. Phys. Chem. B* **2006**, *110*, 3738.

(15) Chen, B.; Siepmann, J. I.; Klein, M. L. *J. Amer. Chem. Soc* **2002**, *124*, 12232.

(16) Wood, W. *J. Chem. Phys.* **1970**, *52*, 729.

(17) Wood, W. W. *J. Chem. Phys.* **1968**, *48*, 415.

(18) Kuo, I. F. W.; Mundy, C. J.; McGrath, M. J.; Siepmann, J. I.; VandeVondele, J.; Sprik, M.; Hutter, J.; Chen, B.; Klein, M. L.; Mohamed, F.; Krack, M.; Parrinello, M. *J. Phys. Chem. B* **2004**,

108, 12990.

(19) Yamaguchi, T.; Hidaka, K.; Soper, A. K. *Mol. Phys.* **1999**, *96*, 1159.

(20) Yamaguchi, T.; Hidaka, K.; Soper, A. K. *Mol. Phys.* **1999**, *97*, 603.

(21) Dang, L. X.; Chang, T. M. *J. Chem. Phys.* **2003**, *119*, 9851.

(22) Handgraaf, J. W.; Meijer, E. J.; Gaigeot, M. P. *J. Chem. Phys.* **2004**, *121*, 10111.

(23) Handgraaf, J. W.; van Erp, T. S.; Meijer, E. J. *Chem. Phys. Lett.* **2003**, *367*, 617.

(24) Mcgrath, M. J.; Siepmann, J. I.; Kuo, I. F. W.; Mundy, C. J. *Mol. Phys.* **2006**, *104*, 3619.

(25) Berghold, G.; Mundy, C. J.; Romero, A. H.; Hutter, J.; Parrinello, M. *Phys. Rev. A* **2000**, *61*, 10040.

(26) Silvestrelli, P. L.; Parrinello, M. *Phys. Rev. Lett.* **1999**, *82*, 3308.

(27) Dang, L. X.; Chang, T. M. *J. Chem. Phys.* **1997**, *106*, 8149.

(28) Kuo, I. F. W.; Mundy, C. J. *Science* **2004**, *303*, 658.

(29) Vuilleumier, R.; Sprik, M. *J. Chem. Phys.* **2001**, *115*, 3454.

(30) Ma, G.; Allen, H. C. *J. Phys. Chem. B* **2003**, *107*, 6343.

(31) Wilson, K. R.; Schaller, R. D.; Co, D. T.; Saykally, R. J.; Rude, B. S.; Catalano, T.; Bozek, J. D. *J. Chem. Phys.* **2002**, *117*, 7738.

(32) Wilson, K. R.; Cavalleri, M.; Rude, B. S.; Schaller, R. D.; Catalano, T.; Nilsson, A.; Saykally, R. J.; Pettersson, L. G. M. *J. Phys. Chem. B* **2005**, *109*.

(33) Wernet, P.; Nordlund, D.; Bergmann, U.; Cavalleri, M.; Odelius, M.; Ogasawara, H.; Naslund, L. A.; Hirsch, T. K.; Ojamae, L.; Glatzel, P.; Pettersson, L. G. M.; Nilsson, A. *Science* **2004**, *304*, 995.

(34) Wick, C. D.; Kuo, I. F. W.; Mundy, C. J.; Dang, L. X. *J. Comput. Theo. Chem.* **2007**, *3*, 2002.